Thermal annealing behaviour and gel to crystal transition of a low molecular weight hydrogelator

Emily C. Barker, Adam D. Martin, Christopher J. Garvey, Ching Yong Goh, Franca Jones, Mauro Mocerino, Brian W. Skelton, Mark I. Ogden and Thomas Becker

SI: Supporting Information

Contents:

Rheology

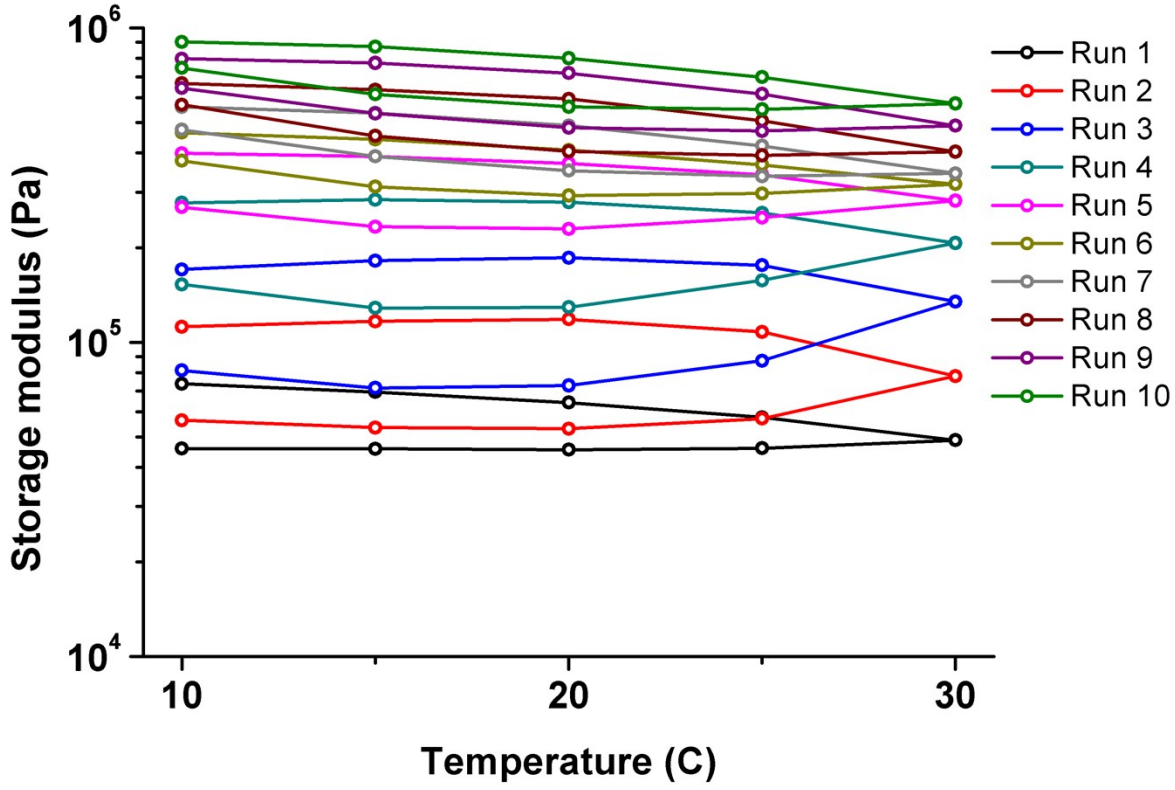

Figure S1 Temperature dependent behaviour of $MgCl_2$·**1** gel. The temperature was cycled ten times between 10 and 30 °C in five degree intervals, with a calixarene concentration of 20 mM used.

Scanning Probe Microscopy

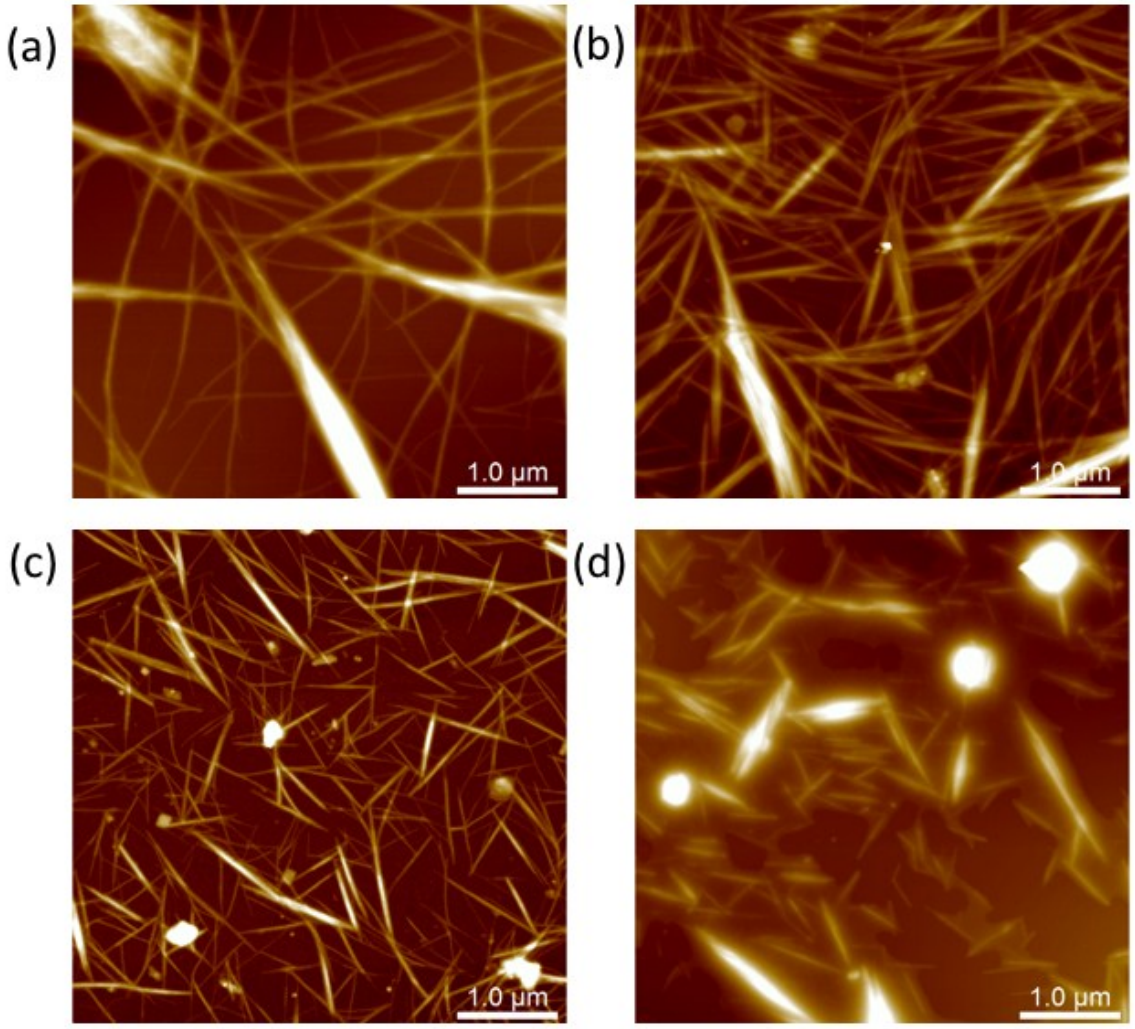

Figure S2. Scanning probe micrographs of a $MgCl_2$·**1** gel imaged *ex situ* smeared on a mica substrate. (a) The gel after initial formation at room temperature. (b) The gel after being heated to 50 ˚C and being allowed to cool to room temperature. (c,d) The gel after one and two more heat cycles respectively.

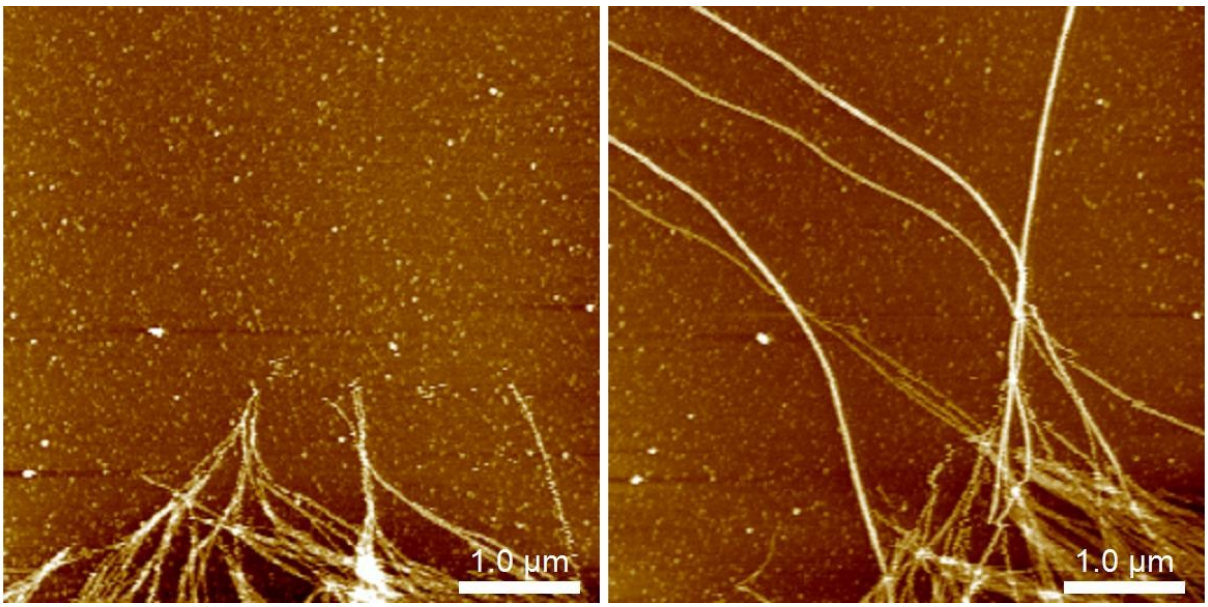

A B

Figure S3. Scanning probe micrographs (topography data) of fibres formed by an aqueous mixture of **1** (20 mM) and LiCl (200 mM) during two consecutive temperature cycles, imaged *in situ*. Scan size: 5 µm; z-scale: 20 nm; 2.1 min/image.

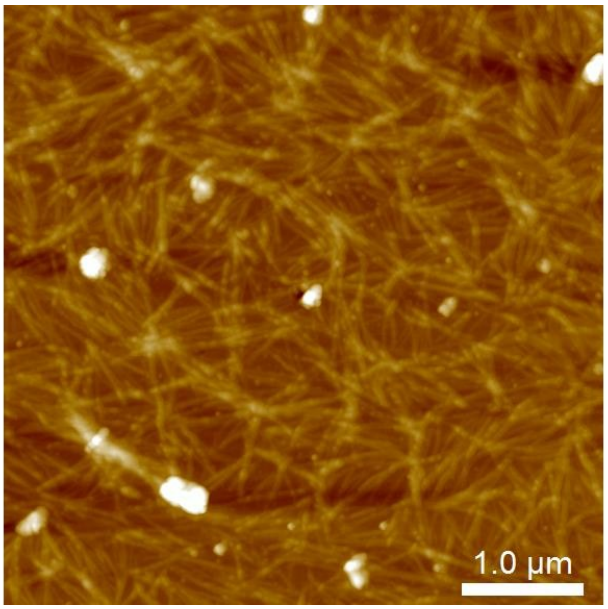

B

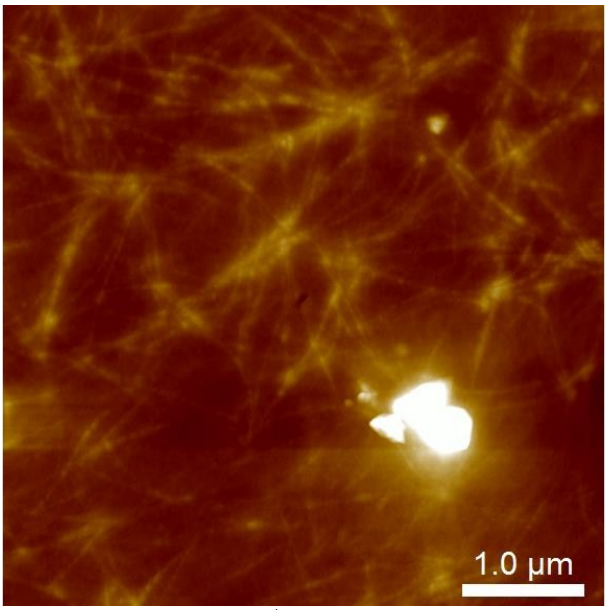

A

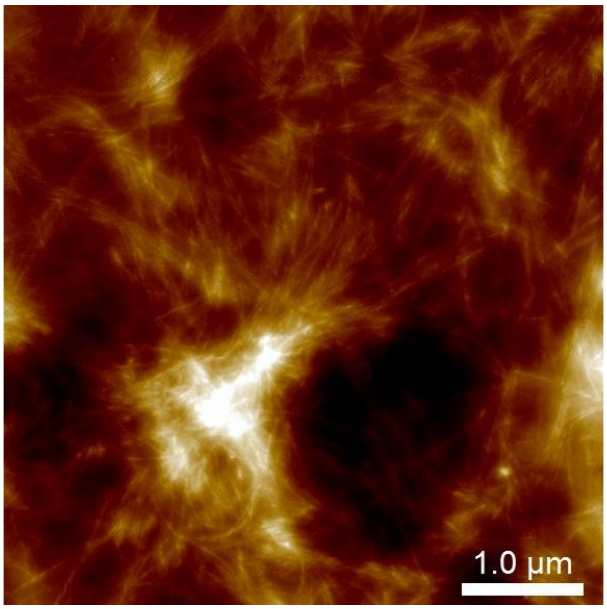

C

Figure S4. Scanning probe micrographs (topography data) of fibres formed by an aqueous mixture of **1** (20mM) and LiCl (1.30M) after consecutive heat cycles, imaged *ex situ*. The sample was heated to 50°C in a water bath and allowed to return to room temperature before smearing a sample on mica for imaging. Images shown are the unheated sample (A), after the sample was heat cycled once (B) and after the sample was heat cycled twice (C). Scan size: 5 µm; z-scale: 35 nm; 8.5 min/image.

SANS refinement details

Small angle scattering data was refined using the flexible cylinder model in SASView. This model was chosen due it being the most physically realistic model for this system, as evidenced through AFM data. For the scattering data at higher temperatures, the flexible cylinder model alone was not sufficient to describe the scattering obtained; therefore a power law fit was also applied at low q values.

Fits were optimised by first calculating the scattering length density (SLD) of the material using the calculator in SASView (for this, a metal:calixarene ratio of 1:1 was used), fixing this and the SLD of the solvent. Other parameters were then allowed to vary freely, and after a few optimisation cycles, the background was fixed. Following this, multiple different starting points were used for the Kuhn length, radius and length of the cylinder, to ensure that a global, physically realistic minimum was found.

SANS model fitting

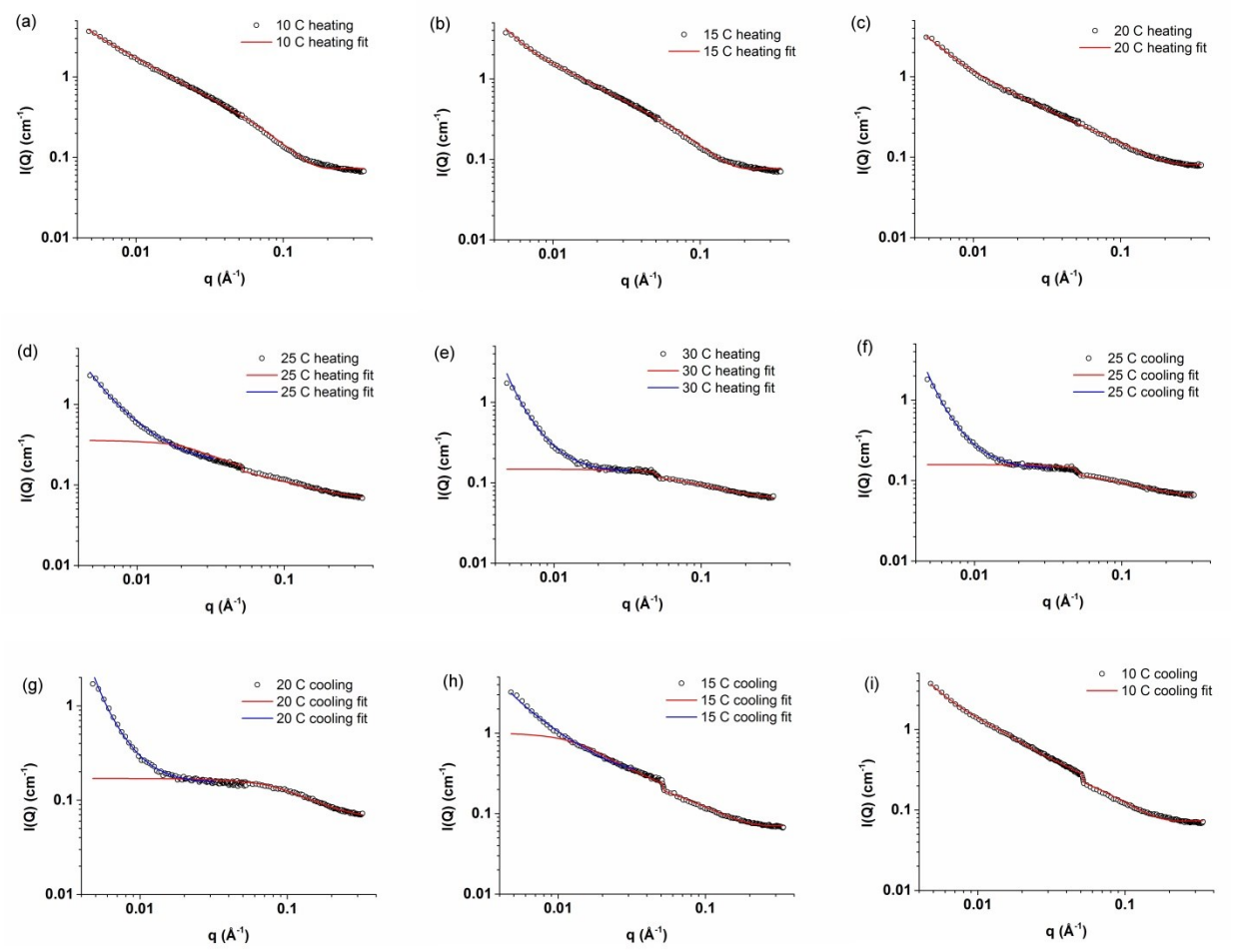

Figure S5 –Model fitting for SANS data of $MgCl_2$·**1** at temperatures studied. Here black dots represent the scattering data, red lines the flexible cylinder model and blue lines the power law model.

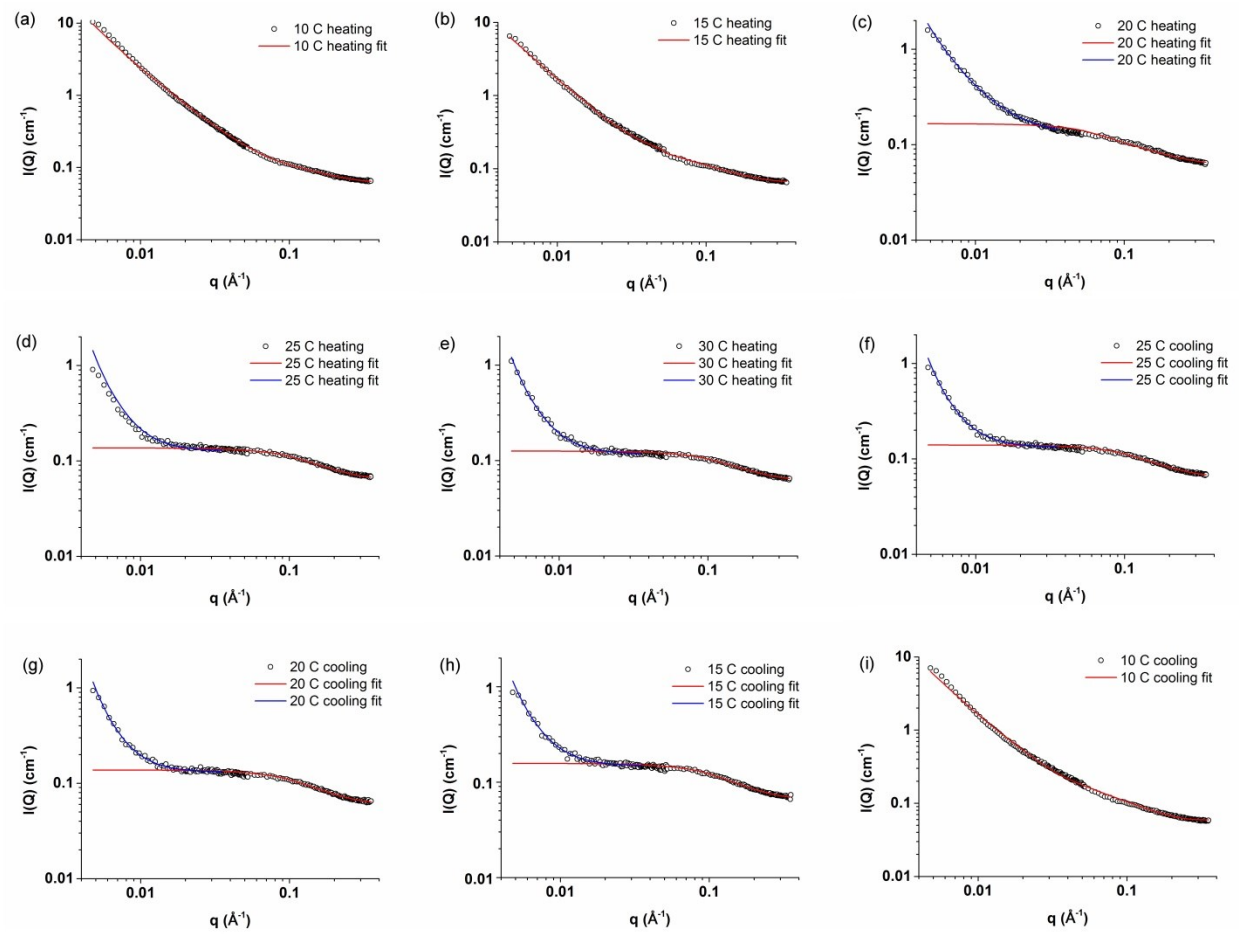

Figure S6 –Model fitting for SANS data of LiCl·**1** at temperatures studied. Here black dots represent the scattering data, red lines the flexible cylinder model and blue lines the power law model.

Table S1 – Fibre radii obtained from model fitting to the data. It should be noted that this is averaged data, and implies that the fibres are of a molecular nature, which stays this way throughout the annealing process

T (°C)	Radius (Å)	Radius (Å)
	1.$MgCl_2$	**1**.LiCl
10	17.3 ± 0.2	8.5 ± 0.1
15	16.5 ± 0.1	9.6 ± 0.1
20	12.2 ± 0.1	8.1 ± 0.1
25	9.5 ± 0.1	8.2 ± 0.3
30	9.5 ± 0.2	7.5 ± 0.5
25	9.5 ± 0.3	8.1 ± 0.1
20	9.5 ± 0.2	8.5 ± 0.3
15	13.6 ± 0.1	8.5 ± 0.3
10	14.6 ± 0.1	11.2 ± 0.4